

# Detection of nuclear magnetic resonance with an anisotropic magnetoresistive sensor

F. Verpillat\*

*Ecole Normale Supérieure de Lyon, 69364 Lyon cedex 07, France*

M. P. Ledbetter<sup>†</sup> and D. Budker<sup>‡</sup>

*Department of Physics, University of California at Berkeley, Berkeley, California 94720-7300*

S. Xu, D. Michalak, C. Hilty, L.-S. Bouchard, S. Antonijevic, and A. Pines

*Department of Chemistry, University of California at Berkeley, Berkeley, California 94720*

(Dated: February 9, 2022)

We report detection of nuclear magnetic resonance (NMR) using an anisotropic magnetoresistive (AMR) sensor. A “remote-detection” arrangement was used, in which protons in flowing water were pre-polarized in the field of a superconducting NMR magnet, adiabatically inverted, and subsequently detected with an AMR sensor situated downstream from the magnet and the adiabatic inverter. AMR sensing is well suited for NMR detection in microfluidic “lab-on-a-chip” applications.

PACS numbers:

The three essential elements of a nuclear-magnetic-resonance (NMR) or magnetic-resonance-imaging (MRI) experiment, nuclear-spin polarization, encoding, and detection can be spatially separated, which is referred to as remote detection of NMR or MRI [1]. One important potential advantage of this approach is that encoding and detection can occur in a near-zero magnetic field; however, conventional inductive detection has poor sensitivity at low frequencies, necessitating the use of alternative techniques for detection. Superconducting quantum-interference devices (SQUIDs) [2] and alkali-vapor atomic magnetometers [3] have been successfully utilized for this purpose. In this note, we report the use of another novel technology – that of anisotropic magneto-resistive (AMR) sensors [4] – for a remote-NMR experiment. Although less sensitive than SQUIDs or atomic magnetometers (including even the miniature chip-scale atomic magnetometers [5]), the all-solid-state AMR sensors do not require cryogenics or vapor-cell heating, and may be particularly fit to microfluidic applications because the sensors are small, inexpensive and can be manufactured as arrays for spatial sensitivity.

The experimental setup is shown in Fig. 1. Tap water, pre-polarized by flowing through a Bruker 17 Tesla magnet, flows through an adiabatic-inversion region, where its polarization is periodically reversed, after which it proceeds to flow past an AMR detector. The adiabatic polarization inverter incorporates a set of coils in anti-Helmoltz configuration to supply a gradient of  $B_z$ . A second set of Helmholtz coils is used to apply a 5.5 kHz oscillating field in the x direction, resonant with the protons’ Larmor frequency in the center of the inverter. When the oscillating field is on, as the water flows through the de-

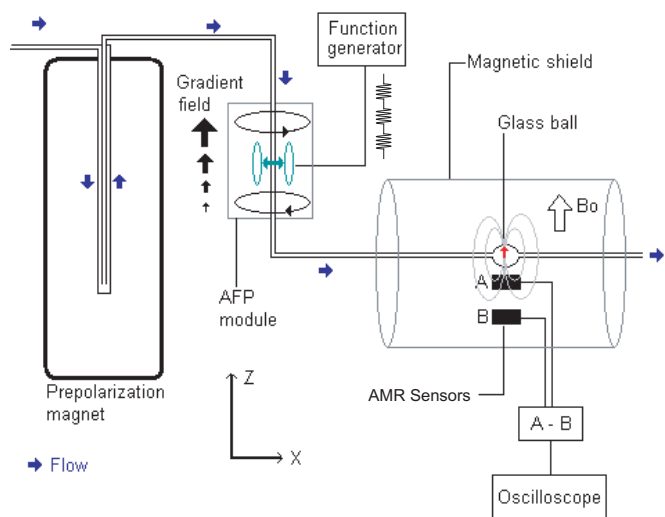


FIG. 1: Experimental setup. Water is pre-polarized by flowing it through the magnet; the magnetization is periodically inverted by passing the liquid through the adiabatic fast passage (AFP) module; the magnetization is detected with a gradiometer consisting of two AMR sensors.

vice, its magnetization is adiabatically reversed. Switching the oscillating field on and off results in magnetization either parallel or anti-parallel to the bias field. After the adiabatic inverter, the water flows into the detection region consisting of a  $0.5\text{--cm}^3$  glass ball adjacent to a pair of Honeywell HMC1001 AMR sensors arranged as a gradiometer in order to cancel the common-mode magnetic-field noise. The active part of the sensor is a thin film with an area of about  $1.5\text{ mm} \times 1.5\text{ mm}$  packaged in a chip with dimensions  $10\text{ mm} \times 3.9\text{ mm} \times 1.5\text{ mm}$ . The manufacturer specifications of the HMC1001 sensor give a single-shot resolution of  $40\text{ }\mu\text{G}$  with a read-out rate of  $1\text{ kHz}$ , corresponding to a sensitivity of about  $1.8\text{ }\mu\text{G}/\sqrt{\text{Hz}}$

\*Electronic address: frederic.verpillat@ens-lyon.fr

<sup>†</sup>Electronic address: ledbetter@berkeley.edu

<sup>‡</sup>Electronic address: budker@berkeley.edu

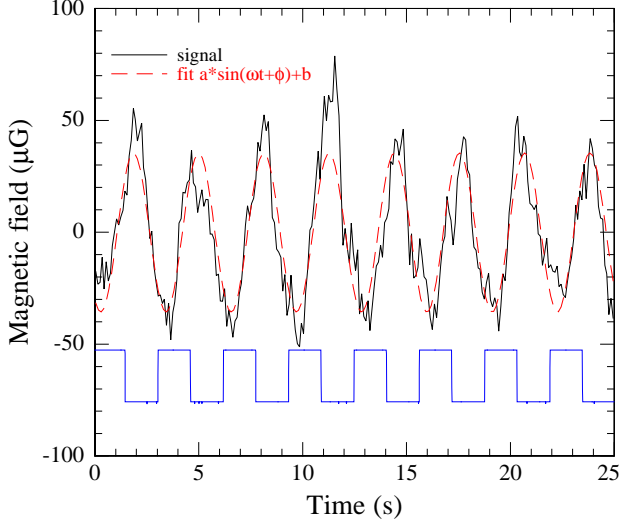


FIG. 2: Upper traces – magnetic field detected with the 0.3 – Hz modulation frequency and a fit to a sinusoidal function. Lower trace – the on-off pattern of the adiabatic inverter. The signal was averaged over 20 min.

assuming white noise. In our experimental setup, we realized a sensitivity of about  $2.7 \mu\text{G}/\sqrt{\text{Hz}}$  at 20 Hz (per sensor), however the low-frequency performance was considerably worse, on the order of  $40 \mu\text{G}/\sqrt{\text{Hz}}$  at 1 Hz, necessitating long signal averaging. The detection region is housed inside a single layer of magnetic shielding with open ends. The water-carrying tube was 1/16" i.d. and the flow rate was  $3.8 \text{ cm}^3/\text{s}$ , corresponding to an average speed of water of  $\approx 2 \text{ m/s}$ . The average travel time from the magnet to the inverter is  $\approx 1.5 \text{ s}$ , and it is  $\approx 0.5 \text{ s}$  from the inverter to the detector.

Data were recorded on a digital oscilloscope, averaging for about 20 min for modulation frequencies in the range 0.3 Hz to 1.7 Hz. There was considerable low-frequency drift in the signal (due to either ambient field drifting or intrinsic drift in the magnetometer) and hence we subtracted from the raw data a slow-varying background approximated by a 3rd-order polynomial. The resulting signal for a modulation frequency of 0.3 Hz is shown in Fig. 2. Neglecting fluid mixing in the transfer tube and detection ball, one would expect that the signal should be a square wave for low modulation frequencies. However, considerable mixing produced signals well approximated (above the cutoff frequency) by a sinusoid, as indicated by the dashed line in Fig. 2.

All the data were fit to sinusoidal profiles and the resulting amplitudes are shown as a function of frequency in Fig. 3. The rapid drop in amplitude is due to mixing of the magnetization as it propagates from the AFP device through the detection ball, effectively integrating the magnetization. A simple model for the spectral response of the system can be obtained in analogy to a low-pass RC filter where the frequency dependence of the signal

is  $S_0 = \alpha M_0 / \sqrt{1 + (f/f_c)^2}$ . Here  $\alpha$  is a proportionality constant depending on geometry relating the magnetic field at the sensor to the magnetization of the sample and  $f_c$  is a cutoff frequency. Overlaying the data in Fig. 3 is a fit to this model function with  $\alpha M_0 = 67 \mu\text{G}$  and  $f_c = 0.2 \text{ Hz}$ .

Significant improvement in sensitivity and bandwidth can be expected in future work. We suspect that the low-frequency performance of our AMR sensor was limited by the open-ended magnetic shields used in the experiment. Optimization of geometry will lead to substantial gains in both sensitivity to nuclear magnetization (by reducing the distance from the sample to the magnetometer), as well as improved bandwidth (by minimizing the volume of the detected water so that less mixing would occur at high frequencies). In principle the detected volume could be a microfluidic channel built into the sensor package, similar to the construction in Ref. [6] where magnetic microparticles were detected. The higher bandwidth has the additional benefit of moving the signal above the  $1/f$  knee of the sensor. Higher sensitivity and spatial resolution may also be achieved by using an array of sensors as in Ref. [7].

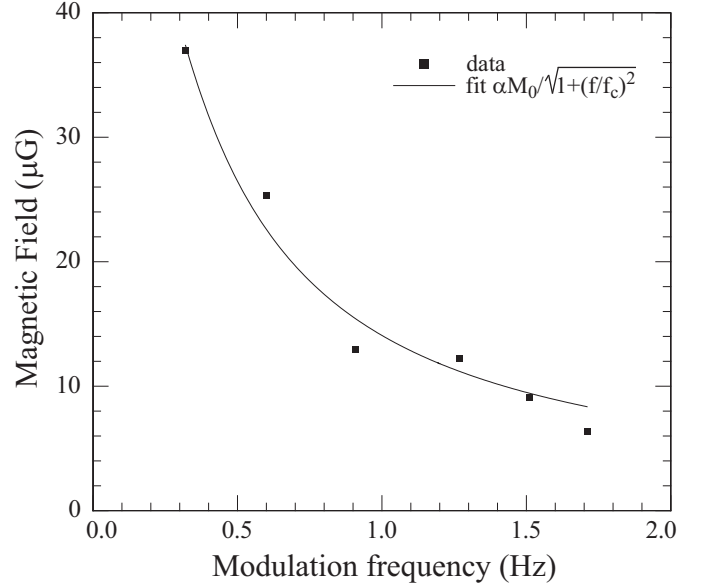


FIG. 3: Amplitude of the modulated water signal and a fit to an RC-filter transfer function.

We have demonstrated, to our knowledge, the first detection of NMR signals using an anisotropic magnetoresistive sensor. The technique may be useful for spatial localization (MRI), relaxometry, diffusometry or spin labeling in chemical analysis [8]. With anticipated future advances in AMR sensors, as well as in related solid-state technologies such as magnetic tunnel junctions, solid-state chip-scale magnetometers may eventually reach the picotesla sensitivity level [9]. Incorporation of built-in microfluidic channels at the chip level will allow the construction of dedicated “lab-on-a-chip” devices. With

these improvements, room temperature, solid state devices appear to be an inexpensive and robust alterna-

tive for detection of both in-situ and remote-detection NMR/MRI without cryogenics.

- 
- [1] A. J. Moulé, M. M. Spence, S. Han, J. A. Seeley, K. L. Pierce, S. Saxena, and A. Pines, *Proc. Natl. Acad. Sci. U. S. A* **100**, 9122 (2003).
  - [2] A. Wong-Foy, S. Saxena, A. J. Moulé, H. M. L. Bitter, J. A. Seeley, R. McDermott, J. Clarke, and A. Pines, *J. Mag. Reson.* **157**, 235 (2002).
  - [3] S. Xu, V. V. Yashchuk, M. H. Donaldson, S. M. Rochester, D. Budker, and A. Pines, *Proc. Natl. Acad. Sci. U. S. A* **103**, 12670 (2006).
  - [4] E. Y. Tsybal and D. G. Pettifor, in *Solid State Physics*, edited by H. Ehrenreich and F. Spaepen (Academic Press, 2001), vol. 56, pp. 113–237.
  - [5] P. D. D. Schwindt, B. Lindseth, S. Knappe, V. Shah, J. Kitching, and L.-A. Liew, *Appl. Phys. Lett.* **90**, 81102 (2007).
  - [6] N. Pekas, M. D. Porter, M. Tondra, A. Popple, and A. Jander, *Appl. Phys. Lett.* **85**, 4783 (2004).
  - [7] D. K. Wood, K. K. Ni, D. R. Schmidt, and A. N. Cleland, *Sensors and Actuators A* **120**, 1 (2005).
  - [8] M. S. Anwar, C. Hilty, C. Chu, L.-S. Bouchard, K. L. Pierce, and A. Pines, *Analytical Chemistry* **79**, 2806 (2007).
  - [9] R. Ferreira, P. Wisniewski, P. P. Freitas, J. Langer, B. Ocker, and W. Maass, *J. Appl. Phys.* **99**, 08K706 (2006).